Synthesis and Structural Characterization of Microporous Framework Zirconium Silicates

Zhi Lin, João Rocha,* Paula Ferreira, and Alan Thursfield

Department of Chemistry, University of Aveiro, 3810 Aveiro, Portugal

Jonathan R. Agger and Michael W. Anderson

Department of Chemistry, UMIST, P.O. Box 88, Manchester, M60 1QD, U.K.

Received: September 14, 1998; In Final Form: November 20, 1998

The synthesis and structural characterization of synthetic analogues of the microporous zirconium silicate minerals petarasite (AV-3), gaidonnayite (AV-4), and umbite (AM-2) are reported. AM-2 materials have been synthesized with different levels of titanium substitution (Zr/Ti molar ratios of ∞,1.9, 0.5, and 0) indicating the existence of a continuous solid solution. All materials have been characterized by several techniques, viz., SEM, powder XRD, single- and triple-quantum ^{23}Na and ^{29}Si MAS NMR, water adsorption measurements, and TGA analysis. As a common structural feature, all these solids possess corner-sharing [ZrO_6] octahedra and [SiO_4] tetrahedra forming a three-dimensional framework. Unlike framework microporous titanosilicates where Ti−O−Ti−O chains are usually present, petarasite, gaidonnayite, umbite, and their synthetic analogues display structures where the [ZrO_6] octahedra are isolated from each other by [SiO_4] tetrahedra and, hence, Zr−O−Zr−O chains do not occur. All these materials are thermally stable up to, at least, 550 °C. The hydration−dehydration processes seem to be reversible.

Introduction

The synthesis of inorganic microporous framework solids containing metal atoms in different coordination geometries has recently attracted considerable interest. We have been particularly concerned with the synthesis and characterization of microporous titanium silicates containing tetracoordinated Si^{4+} and Ti^{4+}, usually in octahedral coordination.[1−3] We are now engaged in a systematic study aimed at preparing novel microporous zirconium silicates. Although several mineral microporous zirconium silicates are known, so far little has been done in order to synthesize such solids in the laboratory. Recently, an excellent example of the interesting and promising chemistry of sodium zirconium silicates has been given by Clearfield and co-workers.[4] We have already briefly reported on the synthesis of AV-3 (Aveiro microporous solid no. 3), a zirconium silicate possessing the structure of the mineral petarasite.[5] We now wish to expound on these studies and to describe the synthesis and structural characterization of synthetic analogues of minerals gaidonnayite and umbite which we have named AV-4 and AM-2 (Aveiro−Manchester microporous solid no. 2), respectively.

Petarasite (Mont St. Hilaire, Québec, Canada) is a rare mineral with the formula $Na_5Zr_2Si_6O_{18}(Cl,OH)\cdot 2H_2O$.[6] Gaidonnayite, with an ideal formula $Na_2ZrSi_3O_9\cdot 2H_2O$, was first found in Mont St. Hilaire in miaroles in nepheline syenite.[7] Umbite is a very rare potassium zirconium silicate which occurs in the Khibiny alkaline massif (Russia).[8] Although the ideal formula of umbite is $K_2ZrSi_3O_9\cdot H_2O$ a pronounced substitution of Ti for Zr occurs. The natural occurrence of purely titaneous umbite is unknown. However, we have previously shown that an analogue of this solid (Ti-AM-2) may be prepared in the laboratory.[2] The successful synthesis of umbite materials with different levels of titanium for zirconium substitution, reported here, indicates the existence of a continuous solid solution which, to our knowledge, has not yet been described for any other sodium or potassium zirconium silicates.

TABLE 1: Bulk Chemical Analysis and TGA Data on AV-3, AV-4, and AM-2 Materials

	AV-3	AV-4	Zr-AM-2	Zr,Ti-AM-2 (1.9)	Zr,Ti-AM-2 (0.5)	Ti-AM-2
Si/(Ti + Zr)	2.91	2.77	2.61	2.44	2.28	3.10
(Na,K)/(Ti + Zr)[a]	2.82	1.96	2.04	1.89	1.82	2.00
mass loss (%)[b]	5.2	9.0	5.1	4.8	5.6	5.0

[a] AV-3 and AV-4 contain Na and Zr, while AM-2 materials contain K, Zr, and Ti. [b] From 30 to 500 °C for AV-4 and AM-2 and from 30 to 800 °C for AV-3.

Experimental Section

Synthesis. The syntheses were carried out in Teflon-lined autoclaves under hydrothermal conditions. In all syntheses, the autoclaves were removed and quenched in cold water after an appropriate time. The off-white microcrystalline powders were filtered, washed at room temperature with distilled water, and dried at 100 °C. Bulk chemical analysis (ICP) data and total mass loss results (from TGA) on these materials are collected in Table 1.

Typical AV-3 Synthesis. An alkaline solution was made by mixing 5.35 g of sodium silicate solution (27% m/m SiO_2, 8% m/m Na_2O, Merck), 7.21 g of H_2O, 1.43 g of NaOH (Merck), 2.00 g of NaCl (Aldrich), and 1.00 g of KCl (Merck). An amount of 0.84 g of $ZrCl_4$ (Aldrich) was added to this solution, and the mixture was stirred thoroughly. The gel, with a composition 1.75 Na_2O:0.28 K_2O:1.0 SiO_2:0.15 ZrO_2:25 H_2O, was autoclaved under autogenous pressure for 10 days at 230 °C.

Typical AV-4 Synthesis. An alkaline solution was made by mixing 4.77 g of sodium metasilicate (Aldrich), 1.40 g of NaOH

* Author to whom correspondence should be addressed.

10.1021/jp983708x CCC: $18.00
Published on Web 01/22/1999

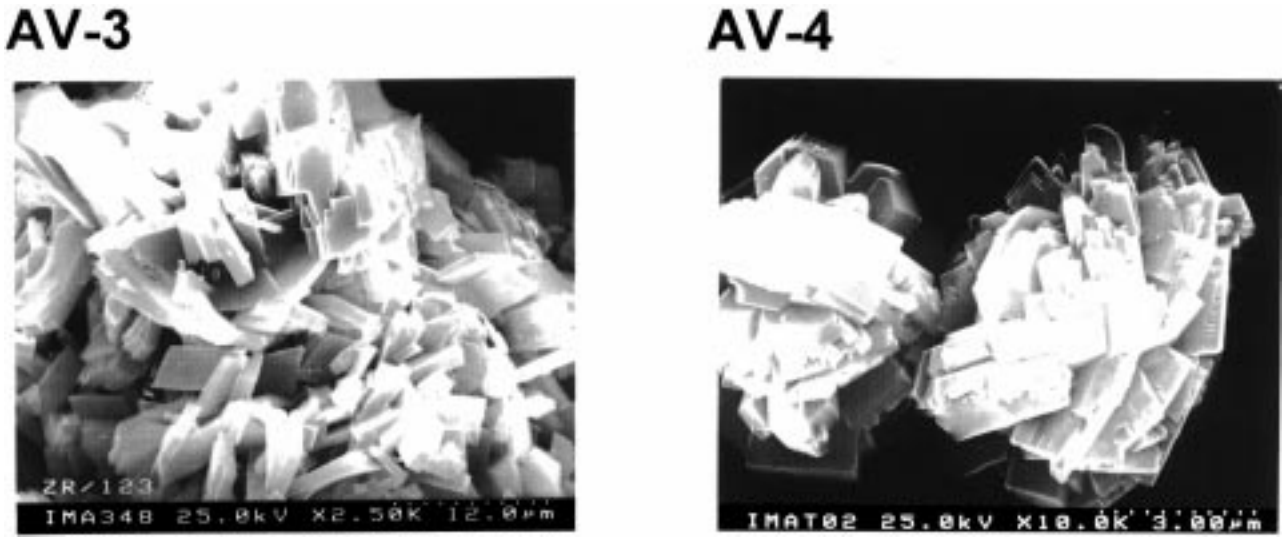

Figure 1. SEM images of AV-3 and AV-4, the synthetic analogues of petarasite and gaidonnayite, respectively.

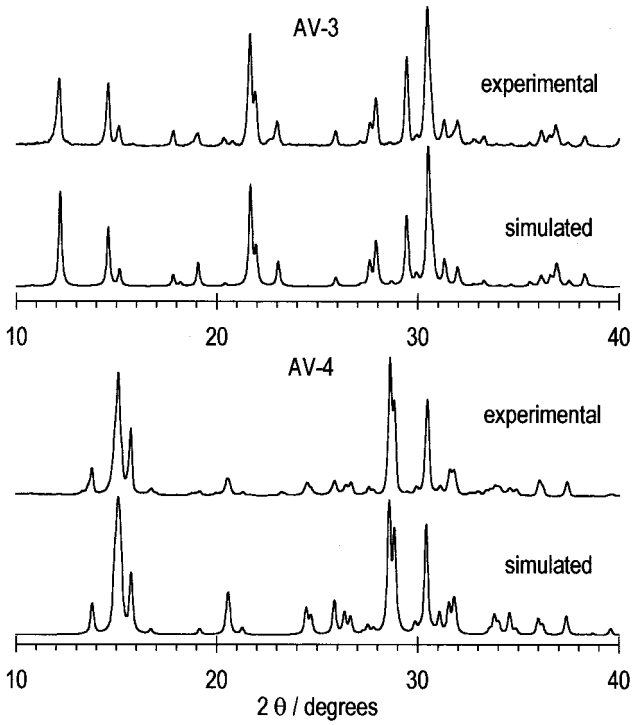

Figure 2. Experimental and simulated powder XRD patterns of AV-3 and AV-4.

(Aldrich), 2.02 g of NaCl (Aldrich), 1.00 g of KCl (Merck), and 14.2 g of H_2O. An amount of 0.88 g of $ZrCl_4$ (Aldrich) was added to this solution, and the mixture was stirred thoroughly. The gel, with a composition 15.2 Na_2O:1.8 K_2O:6.0 SiO_2:1.0 ZrO_2:239 H_2O, was autoclaved under autogenous pressure for 8 days at 200 °C.

Typical AM-2 Syntheses. An alkaline solution was made by mixing 4.20 g of precipitated silica (BDH), 14.08 g of KOH (85% m/m, Aldrich), and 33.4 g of H_2O. An amount of 3.98 g of $ZrCl_4$ (Aldrich) was added to this solution, and the mixture was stirred thoroughly. The gel, with a composition 6.3 K_2O:4.1 SiO_2:1.0 ZrO_2:109 H_2O, was autoclaved under autogenous pressure for 7 days at 230 °C. The synthesis of purely titaneous Ti-AM-2 has been described before.[2] Samples containing Zr and Ti were prepared by introducing Ti (23.5% m/m solution of $TiCl_3$ in 5.9% m/m HCl, Aldrich) into the Zr-AM-2 parent gel to obtain Zr/Ti molar ratios of 0.5 and 2.0.

TABLE 2: Unit Cell Parameters for Mineral and Synthetic Phases

phase	unit cell parameters	ref
petarasite	$a = 10.795$, $b = 14.493$, $c = 6.623$ Å, $\beta = 113.214°$; $V = 953$ Å^3	6
AV-3	$a = 10.771$, $b = 14.505$, $c = 6.575$ Å, $\beta = 112.664°$; $V = 948$ Å^3	*a*
gaidonnayite	$a = 12.820$, $b = 6.691$, $c = 11.740$ Å; $V = 1007$ Å^3	7
AV-4	$a = 12.839$, $b = 6.676$, $c = 11.728$ Å; $V = 1005$ Å^3	*a*
umbite	$a = 10.207$, $b = 13.241$, $c = 7.174$ Å; $V = 970$ Å^3	8
Zr-AM-2	$a = 10.291$, $b = 13.301$, $c = 7.199$ Å; $V = 985$ Å^3	*a*
Zr,Ti-AM-2 (1.9)	$a = 10.197$, $b = 13.220$, $c = 7.179$ Å; $V = 968$ Å^3	*a*
Zr,Ti-AM-2 (0.5)	$a = 10.063$, $b = 13.135$, $c = 7.139$ Å; $V = 944$ Å^3	*a*
Ti-AM-2	$a = 9.935$, $b = 12.977$, $c = 7.128$ Å; $V = 919$ Å^3	*a*

[a] This work.

Techniques. Powder X-ray diffraction (XRD) data were collected on a Rigaku diffractometer using CuKα radiation filtered by Ni. Scanning electron microscope (SEM) images were recorded on a Hitachi S-4100 microscope.

^{23}Na and ^{29}Si NMR spectra were recorded at 105.85 and 79.49 MHz, respectively, on a (9.4 T) Bruker MSL 400P spectrometer. ^{29}Si magic-angle spinning (MAS) NMR spectra were recorded with 40° pulses, spinning rates of 5.0−5.5 kHz, and 40−60 s recycle delays. Chemical shifts are quoted in parts per million from TMS. Single-quantum ^{23}Na MAS NMR spectra were measured using short and powerful radio frequency pulses (0.6 µs, equivalent to a 15° pulse angle), a spinning rate of 15 kHz, and a recycle delay of 2 s. ^{1}H − ^{23}Na cross-polarization (CP) MAS NMR spectra were recorded with a 0.5 ms contact time. Chemical shifts are quoted in ppm from 1 M aqueous NaCl. The triple-quantum (3Q) ^{23}Na MAS NMR spectra[9] were recorded with radio frequency magnetic field amplitudes of ca. 160 kHz. A quantity of 210−256 data points were acquired in the t_1 dimension in increments of 7 µs. To produce pure absorption line shapes in the 3Q MAS spectra the optimum conditions for excitation and transfer of the (±3Q) coherences using a simple two-pulse sequence were used. The phase cycling was composed of six phases for the selection of 3Q coherences. This phase cycling was combined with a classic overall four-phase cycle in order to minimize phase and amplitude mis-settings of the receiver. The ppm scale was referenced to υ_o frequency in the υ_2 domain and to $3\upsilon_o$ in the υ_1 domain (ref 1 M aqueous NaCl).

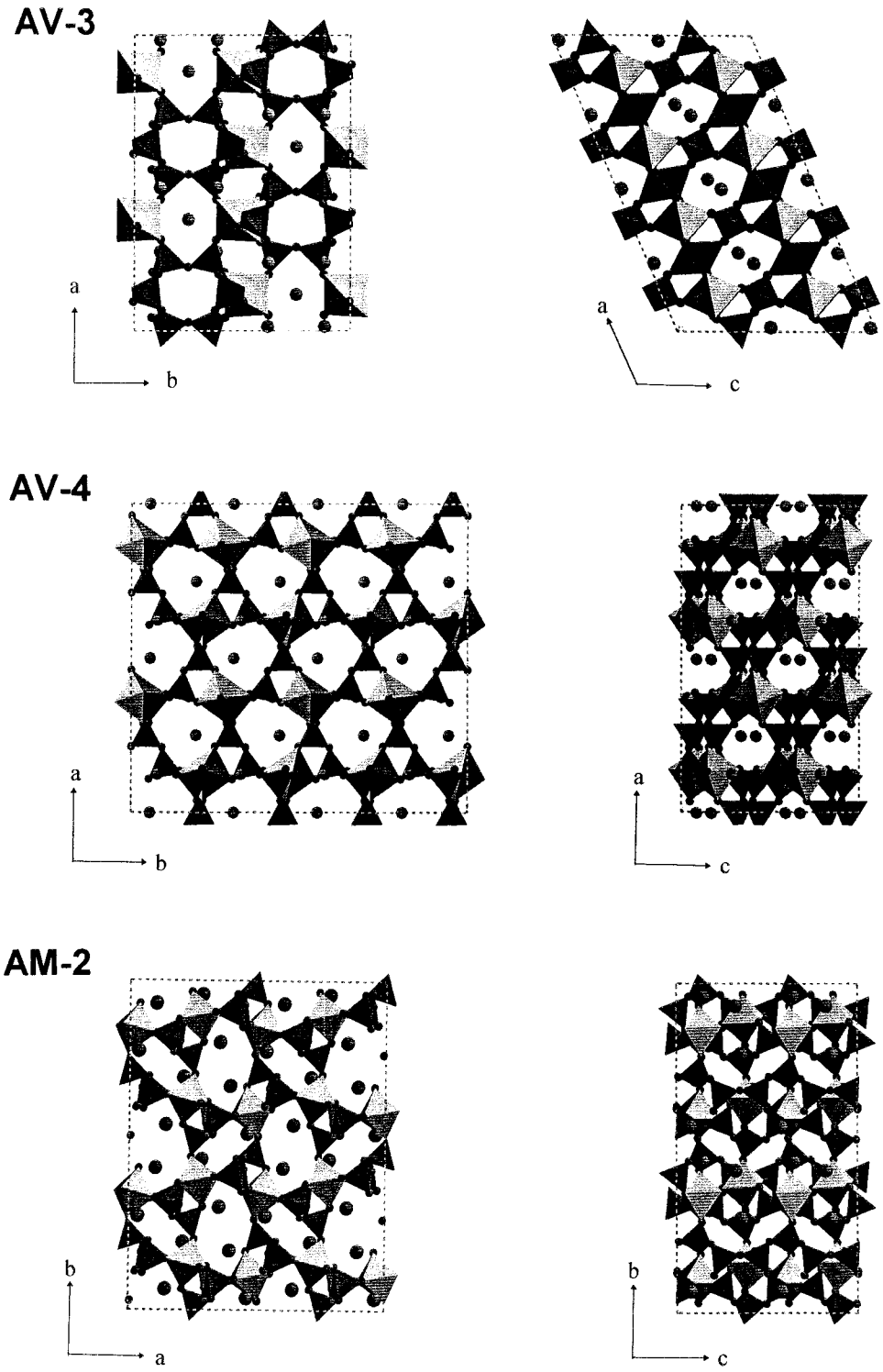

Figure 3. Polyhedral representations of the structures of petarasite (AV-3), gaidonnayite (AV-4), and umbite (AM-2). All materials contain zirconium and silicon ions in octahedral and tetrahedral coordination, respectively.

The adsorption isotherms were measured on a C. I. Instruments electrobalance MK2-M5 connected to a vacuum manifold line. Each sample (ca. 0.1 g) was dehydrated overnight at 450 °C to an ultimate pressure of 10^{-4} mbar and then cooled to room temperature. Diffusion of water was found to be so slow in the samples studied that the adsorption data points were not true equilibrium points. Consequently, an arbitrary time of 60 min was chosen for the delay before each point was recorded. Thermogravimetric (TGA) curves were measured with a TGA-50 analyzer. The samples were heated under air at a rate of 5 °C/min. All materials were routinely characterized by differential scanning calorimetry as well as, Fourier transform infrared, Raman, and diffuse-reflectance ultraviolet spectroscopies, but these data will not be presented here.

Results and Discussion

Scanning Electron Microscopy and Powder X-ray Diffraction. An SEM micrograph and experimental and simulated powder XRD patterns of synthetic petarasite (AV-3) are shown in Figures 1 and 2, respectively. The unit cell parameters of AV-3, given in Table 2, have been calculated assuming a

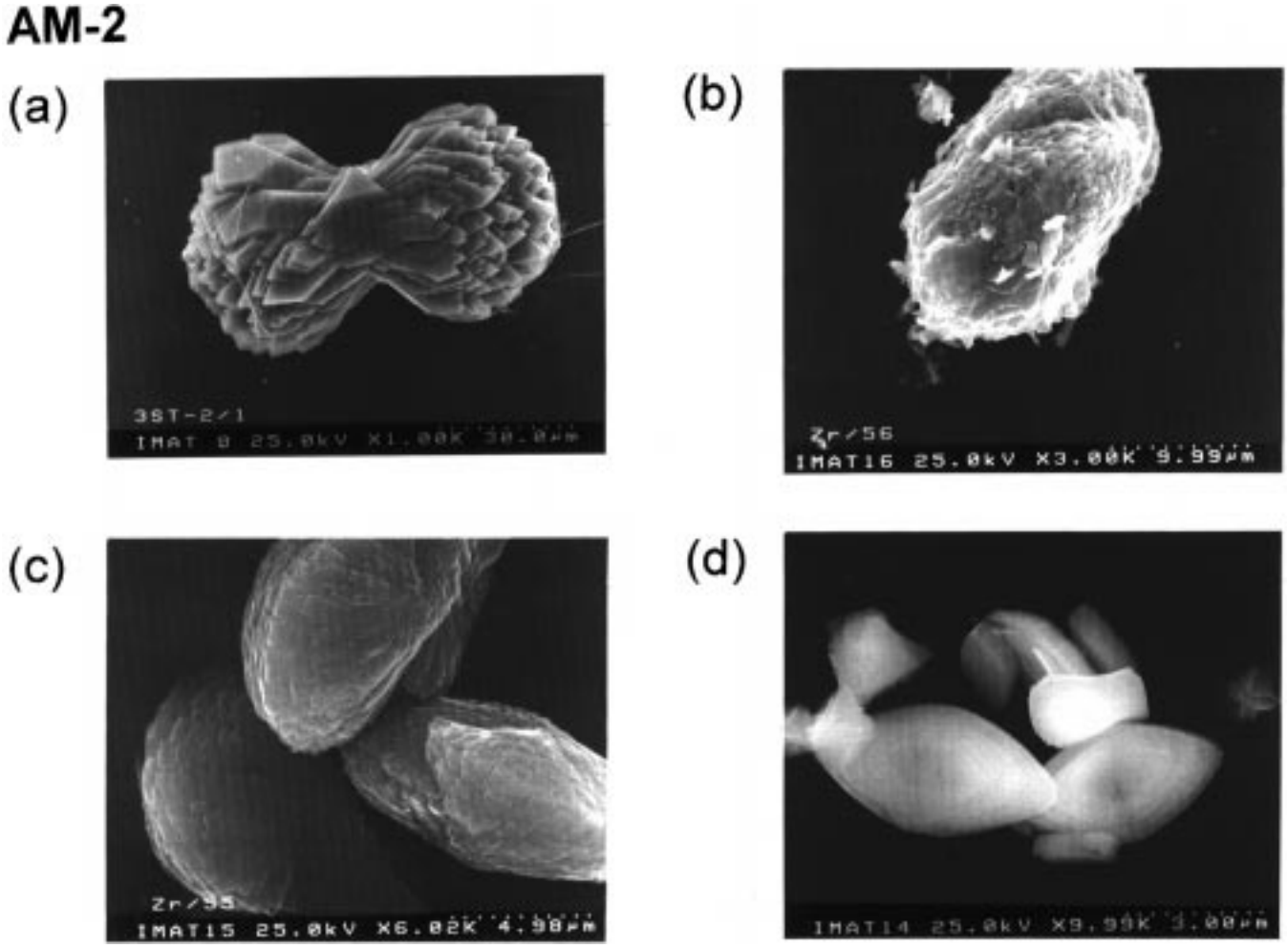

Figure 4. SEM images of synthetic umbite (AM-2) materials: (a) purely titaneous sample, (b) Zr/Ti = 0.5, (c) 1.9, and (d) purely zirconeous sample.

monoclinic unit cell, space group $P2_1/m$, and are similar to those reported for petarasite.[6] The crystal structure of petarasite (and AV-3) consists of an open three-dimensional framework built of corner-sharing six-membered silicate rings and [ZrO_6] octahedra (Figure 3).[6] Elliptical channels (3.5 × 5.5 Å) defined by mixed six-membered rings, consisting of pairs of [SiO_4] tetrahedra linked by Zr octahedra, run parallel to the *b*- and *c*-axes. Other channels limited by six-membered silicate rings run parallel to the *c*-axis. The sodium, chloride, and hydroxyl ions and the water molecules reside within the channels.

An SEM micrograph and experimental and simulated powder XRD patterns of synthetic gaidonnayite (AV-4) are shown in Figures 1 and 2, respectively. The unit cell parameters have been calculated assuming an orthorhombic unit cell, space group $Pna2_1$, and are similar to those reported for gaidonnayite.[7] The framework of gaidonnayite (and AV-4) (Figure 3) is composed of sinusoidal single chains of [SiO_4] tetrahedra, repeating every six tetrahedra.[7] The chains extend alternately along [011] and [$01\bar{1}$] and are cross-linked by a [ZrO_6] octahedron and two distorted [NaO_6] octahedra.

SEM micrographs of Zr,Ti-AM-2 materials (Figure 4) show that the crystal morphology and size changes considerably with the Zr/Ti molar ratio. Figure 5 shows experimental and simulated powder XRD patterns of AM-2 materials, while Table 2 depicts the unit cell parameters refined using 23 well-resolved reflections and compares these with the parameters reported for mineral umbite.[8] These simulations were carried out using occupancy factors derived from the Zr/Ti ratios obtained by bulk chemical analysis. It is clear that with increasing substitution of Ti for Zr the unit cell shrinks in the three directions and its volume decreases systematically. This is not unexpected because Ti(IV) is smaller than Zr(IV). In the structure of umbite (Figure 3) the M octahedra, [(Zr,Ti)O_6], and T tetrahedra, [SiO_4], form a three-dimensional MT-condensed framework.[8] The M octahedron is coordinated to six T tetrahedra and, therefore, does not form M−O−M chains. In addition to the M−O−T bonds these tetrahedra also form T−O−T links with each other. The resulting T radical has an identity period of three T tetrahedra and forms an infinite chain. Among all the known silicates and their T analogues, the umbite structure seems to be the first one to display such an MT-condensed framework.[8]

^{29}Si and ^{23}Na Solid-State NMR. The AV-3 ^{29}Si solid-state MAS NMR spectrum (Figure 6) displays three peaks at −86.6, −91.9, and −94.3 ppm in a 1:0.9:1 intensity ratio. In accord with this observation, the crystal structure of petarasite calls for the presence of three unique Si sites with equal populations.[6]

The sheared ^{23}Na 3Q MAS NMR spectrum of AV-3 (Figure 7) contains two resolved peaks at ca. 5.9 and 2.4 ppm F1 and, due to a distribution of isotropic chemical shifts, a relatively broad signal centered at ca. 9.6 ppm F1. From the centers of gravity δ_1 and δ_2 (F_1 and F_2 dimensions, respectively) of the two-dimensional spectrum it is possible to estimate the (average) isotropic chemical shift δ_{iso} and the SOQE parameter of the lines:[10] S1 (−3.9 ppm, 2.1 MHz), S2 (−1.9 ppm, 2.5 MHz), and S3 (−1.4 ppm, 3.1 MHz). Petarasite contains three crystallographically independent seven-coordinated sodium

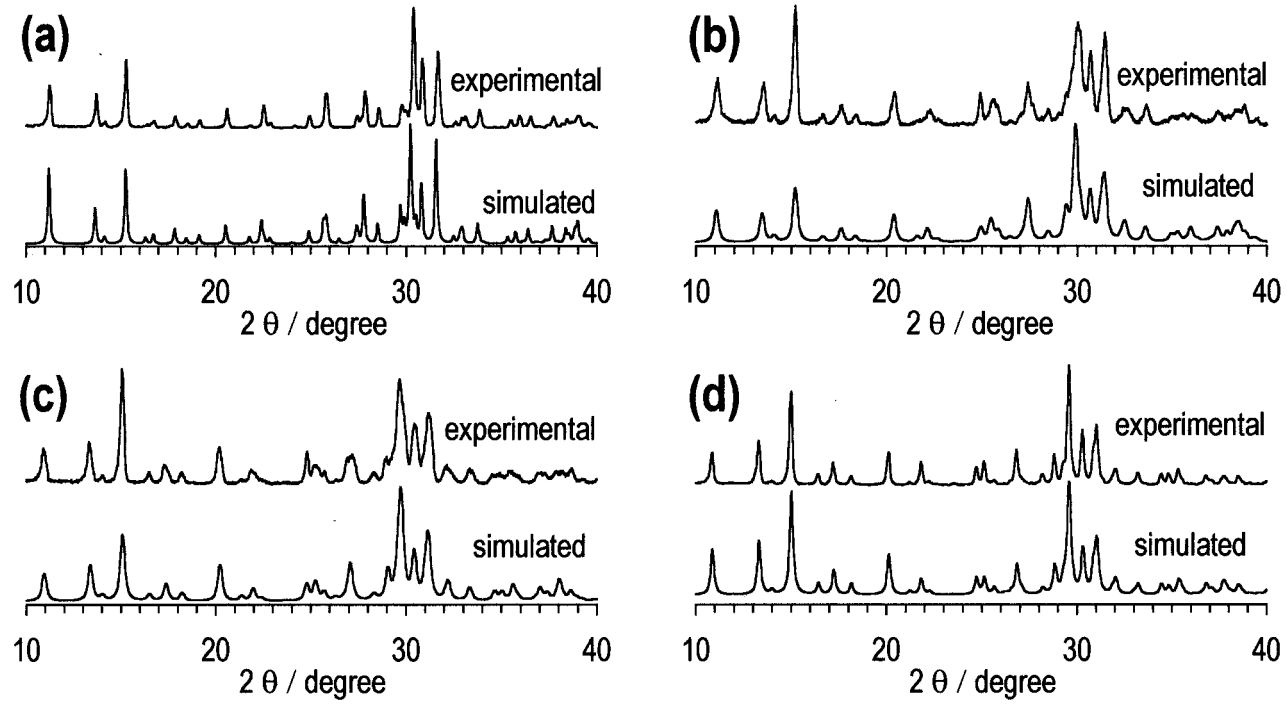

Figure 5. Experimental and simulated powder XRD patterns of synthetic umbite (AM-2) materials: (a) purely titaneous sample, (b) Zr/Ti = 0.5, (c) 1.9, and (d) purely zirconeous sample.

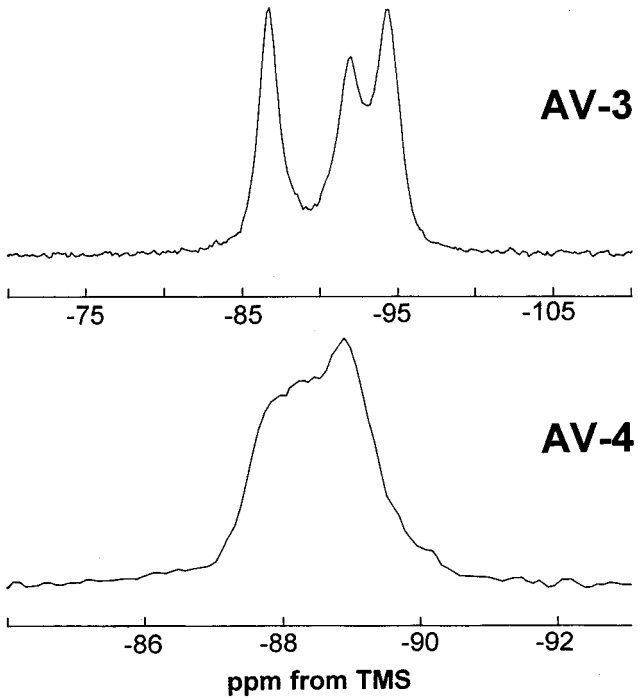

Figure 6. ^{29}Si MAS NMR spectra of AV-3 and AV-4.

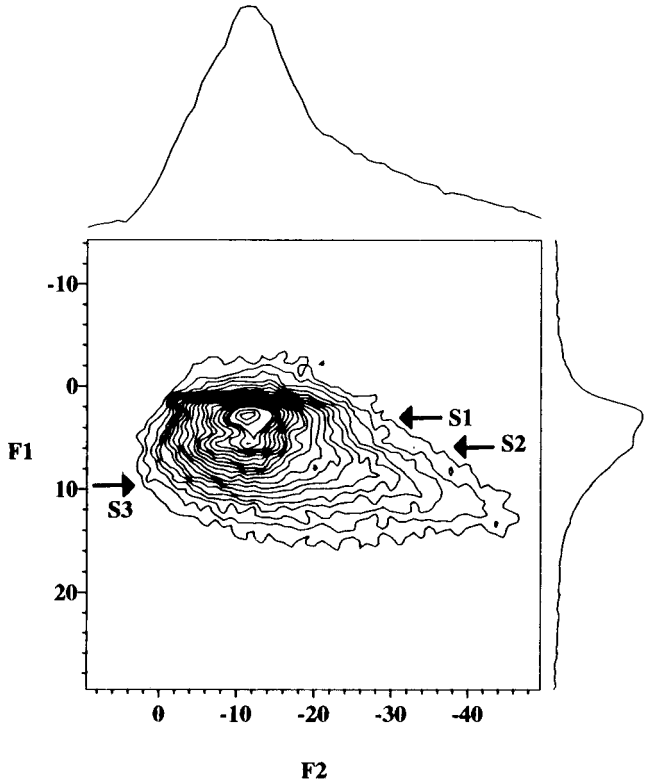

Figure 7. Sheared 3Q ^{23}Na MAS NMR spectrum of AV-3.

sites.[6] Na(1) and Na(2) reside in channels parallel to *b*, and Na(3) is located in channels parallel to *c*. The [Na(1)O_5(H_2O)-Cl] and [Na(2)O_5(H_2O)Cl] polyhedra are distorted monocapped octahedra, while the [Na(3)O_6Cl] polyhedron is a distorted hexagonal pyramid. A second Cl atom may be considered part of the Na(3) coordination and this is, thus, the most distorted sodium site. Accordingly, peak S3, which displays the largest SOQE, is attributed to site Na(3). This assignment is supported by ^{1}H − ^{23}Na cross-polarization (CP) MAS NMR spectroscopy (Figure 8). The broad low-frequency tail seen in the single-quantum ^{23}Na MAS NMR spectrum, which is due to peak S3 (see F2 projection in Figure 7), is not present in the CP/MAS NMR spectrum. Such behavior is expected for Na(3) because the site is not coordinated to any water molecules. In contrast, sites Na(1) and Na(2), which have water molecules in their coordination spheres, cross-polarize relatively well. The quantification of the MQ MAS NMR spectra is not a trivial problem. Indeed, the intensity of the resonances is not representative of the actual concentration of species because the excitation of the MQ coherences is strongly dependent on the NMR quadrupole frequency. However, since we have recorded the ^{23}Na

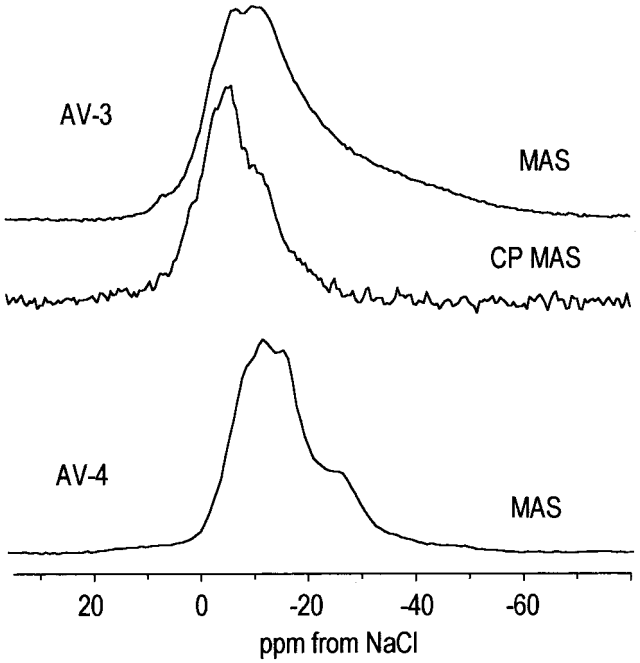

Figure 8. Single-quantum ("normal") ^{23}Na MAS NMR spectra of AV-3 and AV-4. The ^{1}H − ^{23}Na CP/MAS NMR spectrum of AV-3 is also shown.

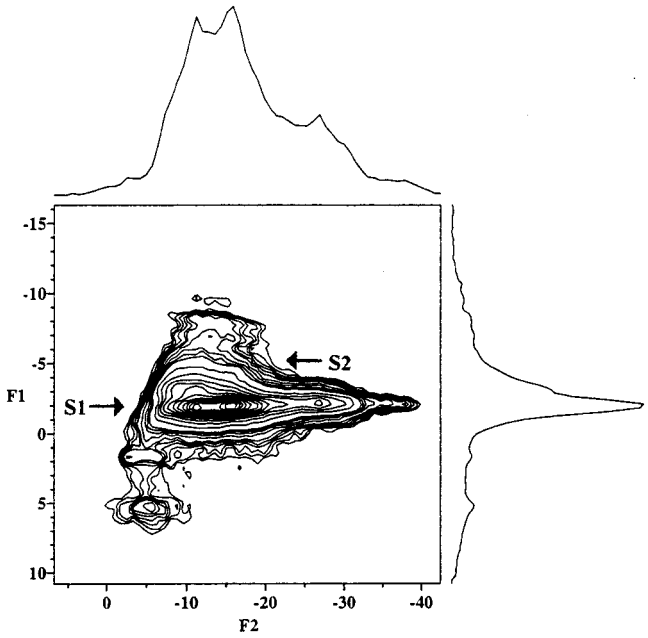

Figure 9. Sheared 3Q ^{23}Na MAS NMR spectrum of AV-4.

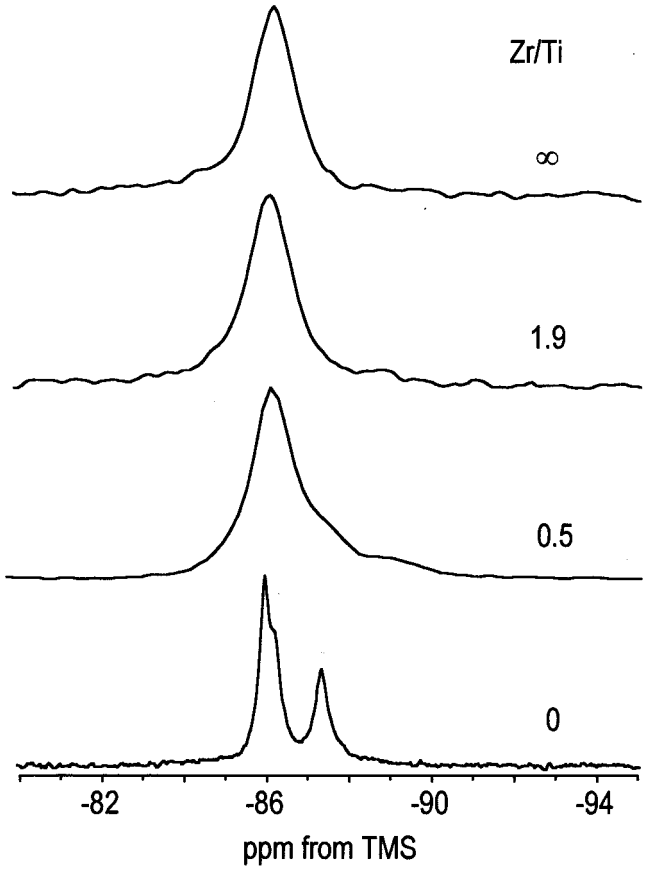

Figure 10. ^{29}Si MAS NMR spectra of AM-2 materials.

MAS NMR spectrum of AV-3 with a strong (160 kHz) radio frequency field we believe the measured peak intensities are approximately correct. These have been derived by both volume integration and deconvolution of the isotropic (F1) sum projections. These methods yield for S1, S2, and S3 intensity ratios of 1.0:1.0:0.8−0.9, respectively, in good agreement with the crystal structure of petarasite.

The AV-4 ^{29}Si MAS NMR spectrum (Figure 6) displays a main peak at −88.8 ppm and two strongly overlapping peaks at ca. −88.2 and −87.8 ppm in a ca. 1:1:1 intensity ratio (as revealed by deconvolution of the spectrum). In accord with this observation, the crystal structure of gaidonnayite calls for the presence of three unique Si(2Si, 2Zr) sites with equal populations.[7]

Gaidonnayite contains two independent Na sites.[7] Both Na(1) and Na(2) are coordinated with four oxygen atoms and two water molecules to form a highly distorted octahedron. The water molecules are located at opposite corners in the (most distorted) Na(1)−O octahedron and on adjacent corners in the Na(2) octahedron. The Na−H_2O bonds are significantly shorter than the Na−O bonds in both octahedra. The single-quantum ^{23}Na MAS NMR spectrum of AV-4 (Figure 8) contains a broad peak centered at about −10 ppm. The sheared ^{23}Na 3Q MAS NMR spectrum of AV-4 (Figure 9) contains a main (S1) resonance at −2 ppm F1 with a relatively large SOQE of 2.1 MHz and a δ_{iso} of −8.0 ppm, consistent with sodium atoms in highly distorted environments. A second (S2) peak, with a much smaller SOQE of 1.6 MHz and a δ_{iso} of −7.9 ppm is seen at ca. −3.5 ppm F1. The spectrum displays, at least, two other faint resonances at about 5.5 and −7 ppm F1. To estimate the relative contributions of peaks S1 and S2, we have attempted to simulate the single-quantum ^{23}Na MAS NMR spectrum (not shown). Although we could not achieve a perfect agreement between the simulated and the experimental spectra, it was possible to conclude that the S1/S2 intensity ratio is, at least, 5:1. Thus, it is likely that S2 and the other faint signals are given by unknown impurities, rather than by one of the AV-4 sodium sites.

The ^{29}Si MAS NMR spectra of AM-2 materials are shown in Figure 10. In the structure of umbite there are three types of Si(2Si, 2Zr) sites with populations 1:1:1.[8] The spectrum of Zr-AM-2 displays a single broad peak at −86.5 ppm. In contrast, the spectrum of the purely titaneous sample contains a resonance at −87.3 ppm and two overlapping peaks at about −86.2 and −85.9 ppm in ca. 1:1: 1 intensity ratio,[2] in accord with the crystal structure of umbite.[8] Along the series, it is observed that as the Zr content of the samples increases the peak at about −86.5 ppm broadens while the resonance at −87.3 ppm

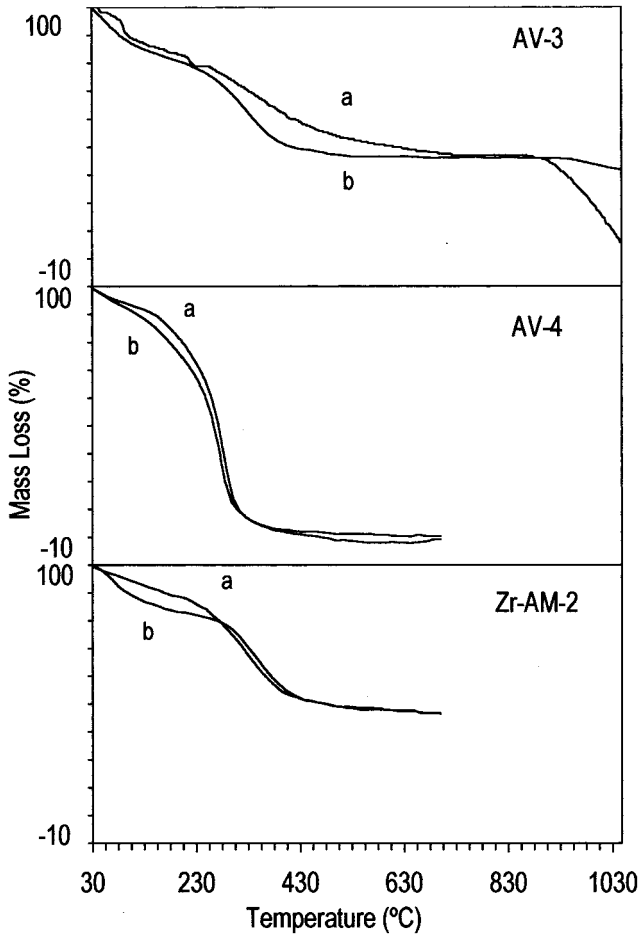

Figure 11. TGA curves of (a) as-prepared AV-3, AV-4, and AM-2 materials; and (b) materials after the first dehydration cycle (500 °C for AV-4 and AM-2, 750 °C for AV-3) and overnight rehydration at room temperature.

broadens and eventually disappears from the spectrum. This observation further suggests the isomorphous substitution of Ti for Zr in synthetic umbite.

Water Adsorption Isotherms. The end members of the AM-2 series were studied and give a distorted type I water adsorption isotherm (not shown) with a small continuous increase in mass beyond $P/P° = 0.2$, instead of the characteristic plateau region of constant mass with increasing overpressure. Adsorption was found to be slow, presumably because of the small pore sizes and the presence of potassium ions within the pores. Indeed, 9 h of experimental time was required for ca. 6% of water to be taken up at $P/P° = 1$. AV-4 also gives a type I adsorption isotherm due to slow adsorption (not shown), although it achieved a higher uptake (ca. 9%) than the AM-2 materials at $P/P° = 1$. AV-3 (not shown) displays a very small (less than 1% at $P/P° = 0.8$) water uptake and a complex adsorption isotherm, resembling type III more than type I. This behavior fits with the low water uptake (as type III isotherms are associated with very weak adsorbent−adsorbate interactions). However, as the data points were not obtained at equilibrium and the presence of sodium and chloride species within the pores may drastically increase the equilibrium time of each data point, the observed type III-like isotherm may be an extreme distortion of a type I isotherm.

Thermal Stability. TGA (Figure 11) provides further evidence that the structures of AV-3 and petarasite are very similar. The total mass loss between 30 and 800 °C is 5.3% and is due to the release of molecular water, structural or adsorbed. This value corresponds to 2.4 water molecules and is in excess of the two water molecules revealed by the crystal-structure analysis. Thus, as petarasite,[11] the solid contains a considerable amount of adsorbed water. Between ca. 800 and 1050 °C a second stage of dehydration occurs with a mass loss of 3.1% (3.19% in petarasite corresponding to $[Cl_{0.67}(OH)_{0.33}]$), probably due to the loss of Cl and OH. The parent AV-3 and the material calcined at 750 °C and rehydrated in air overnight at room temperature display similar TGA curves (Figure 11) and powder XRD patterns (not shown). The fact that the framework does not collapse until the release of Cl indicates that this is an essential constituent of the structure.[11]

The mass loss of AV-4 (from 30 to 500 °C) is ca. 9.0%. TGA (Figure 11) and powder XRD (not shown) indicate that the structure is preserved upon dehydration (9.25% reported for gaidonnayite[12]). The mass losses of the Zr,Ti-AM-2 materials (from 30 to 500 °C) are between 4.8 and 5.6%. The typical TGA curve of synthetic umbite show that the water loss is reversible. Most of the water is lost between 250 and 400 °C. The powder XRD patterns of our AM-2 materials calcined at 550 °C show that the samples are only slightly less crystalline than the parent materials.

Conclusion

In this paper the preparation and structural characterization of synthetic analogues of the minerals petarasite (AV-3), gaidonnayite (AV-4), and umbite (Zr, Ti-AM-2) have been reported. AM-2 materials have been synthesized with different levels of titanium substitution (Zr/Ti molar ratios of ∞,1.9, 0.5, and 0) indicating the existence of a continuous solid solution which, to our knowledge, has not yet been reported for any other sodium or potassium zirconium silicates. A common structural feature of these solids is that they all possess corner-sharing $[ZrO_6]$ octahedra and $[SiO_4]$ tetrahedra forming a three-dimensional framework. Interestingly, unlike framework microporous titanosilicates where Ti−O−Ti−O chains are usually present, microporous zirconium silicates display framework structures where the $[ZrO_6]$ octahedra are isolated from each other by $[SiO_4]$ tetrahedra and, hence, in general Zr−O−Zr−O chains do not seem to occur. All materials are thermally stable up to, at least, 550 °C. The hydration−dehydration processes seem to be reversible.

Acknowledgment. The Portuguese team thanks FEDER and PRAXIS XXI for financial support.

References and Notes

(1) Anderson, M. W.; Terasaki, O.; Ohsuna, T.; Phillippou, A.; Mackay, S. P.; Ferreira, A.; Rocha, J.; Lidin, S. *Nature* **1994**, *367*, 347.

(2) Lin, Z.; Rocha, J.; Brandão, P.; Ferreira, A.; Esculcas, A. P.; Pedrosa de Jesus, J. D.; Philippou, A.; Anderson, M. W. *J. Phys. Chem. B* **1997**, *101*, 7114.

(3) Dadachov, M. S.; Rocha, J.; Ferreira, A.; Lin, Z.; Anderson, M. W. *Chem. Commun.* **1997**, 2371.

(4) Bortun, A. I.; Bortun, L. N.; Clearfield, A. *Chem. Mater.* **1997**, *9*, 1854.

(5) Rocha, J.; Ferreira, P.; Lin, Z.; Agger, J. R.; Anderson, M. W. *Chem. Commun.* **1998**, 1269.

(6) Ghose, S.; Wan, C.; Chao, G. Y. *Can. Mineral.* **1980**, *18*, 503.

(7) Chao, G. Y. *Can. Mineral.* **1985**, *23*, 11.

(8) Ilyushin, G. D. *Inorg. Mater.* **1993**, *29*, 853.

(9) Medek, A.; Harwood: J. S.; Frydman, L. *J. Am. Chem. Soc.* **1995**, *117*, 12779.

(10) Fernandez, C.; Amoureux, J. P.; Chezeau, J. M.; Delmotte, L.; Kessler, H. *Microporous Mater.* **1996**, *6*, 331.

(11) Chao, G. Y.; Chen, T. T.; Baker, J. *Can. Mineral.* **1980**, *18*, 497.

(12) Chao, G. Y.; Watkinson, D. H. *Can. Mineral.* **1974**, *12*, 316.